6

Fine Synchronization in UWB Ad-Hoc Environments

Moez Hizem and Ridha Bouallegue
6'Tel/Sup'Com, University of Carthage
Tunisia

1. Introduction

UWB impulse radios (UWB-IR) have attracted increasing interest due to their potential to propose high user capacity with low-complexity and low-power transceivers (Win & Sholtz, 2000). It is approved by the Federal Communications Commission's (FCC) Report in which the UWB spectral mask is released and published in February 2002. Most of these benefits initiate from the distinctive characteristics inherent to UWB wireless transmissions (Yang & Giannakis, 2004). These make UWB connectivity appropriate for indoor and especially short-range high-rate wireless environments, as well as for strategic outdoor communications. However, to harness these benefits, one of the most critical challenges is the synchronization step and more specifically timing offset estimation. Bit error rate (BER) analysis also exposes evident performance degradation of UWB radios due to mistiming (Tian & Giannakis, 2005). The complexity of which is accentuated in UWB owing to the fact that information bearing waveforms are impulse-like and have low amplitude. In addition, compared to narrowband systems, the difficulty of timing UWB signals is increased further by the dense multipath channel that remains unknown at the synchronization step. These reasons give explanation why synchronization has obtained so much importance in UWB research (Fleming et al, 2002; Homier & Sholtz, 2002; Tian & Giannakis, 2003; Yang et al, 2003).

Typically, pulse position modulation (PPM), pulse amplitude modulation or on/off keying (OOK) is employed. PPM modulation transmits pulses with constant amplitude and encodes the information according to the position of the pulse, while PAM and OOK use the amplitude for this purpose. Moreover, PPM is regularly implemented to reduce transceiver complexity in UWB systems. But unlike pulse amplitude modulation (PAM) applied in the context of UWB systems, the difficulty of accurate synchronization is accentuated in PPM UWB systems owing to the fact that information is transmitted by the shifts of the pulse positions.

In the last years, numerous timing algorithms have been studied for UWB impulse radios under various operating environments. Least squares (LS) (Carbonelli et al, 2003) and Maximum-likelihood (ML) approaches (Lottici et al, 2002) are available, but tend to be computationally complex as they need high sampling rates. In (Djapic et al, 2006), a blind synchronization algorithm that takes advantage of the shift invariance structure in the frequency domain is proposed. An accurate signal processing model for a Transmit-reference UWB (TR-UWB) system is given in (Dang et al, 2006). The model considers the

channel correlation coefficients that can be estimated blindly. In (Ying et al, 2008), the authors proposed a code-assisted blind synchronization (CABS) algorithm which relies on the discriminative nature of both the time hopping code and a well-designed polarity code. Timing with dirty templates (TDT), which is the starting point of this paper, was introduced in (Yang & Giannakis, 2005) for rapid synchronization of UWB signals and was developed in (Yang, 2006) for PPM-UWB signals with direct sequence (DS) and/or time hopping (TH) spreading. This technique is based on correlating adjacent symbol-long segments of the received waveform. TDT is functional with random and unknown transmitted symbol sequences. When training symbols are approachable, the performance of the TDT synchronizer can be improved by approving a data-aided (DA) mode (Yang & Giannakis, 2005). The DA mode significantly outperforms the non-data-aided (NDA) one. However, the training sequences require an overhead which reduces the bandwidth and energy efficiency. Except (Yang, 2006), all these timing algorithms are developed for PAM-UWB signals. Since their operations greatly rely on zero-mean property of PAM, these presented timing algorithms are not appropriate to PPM-UWB signals.

In this chapter, to address and try to solve the problem of synchronization for Ultra Wideband (UWB) systems in ad-hoc environments, we propose a fine synchronization algorithm for PAM and PPM UWB signals with a spread spectrum involving Time Hopping (TH). We adopt first a blind (or coarse) synchronization technique, which is Timing with dirty templates (TDT). Its principle is to correlate two consecutive symbol-long segments of the received waveform. In particular, synchronization will be asserted when the correlation function reaches its maximum. This allows TDT algorithms to effectively collect the multipath energy even when the spreading codes and the channel are both unknown. However, this technique estimates coarsely (or roughly) the value of timing offset, therefore not precisely, and this may cause a shortfall in performance of our UWB impulse radio systems. To improve synchronization performance of the TDT (Timing with Dirty Templates) algorithm developed in mentioned papers, our contribution will be to implement a new fine synchronization stage and place it after the dirty one, which is TDT approach. The principle of our fine synchronization algorithm is to make a fine research in order to find the exact moment of the beginning pulse (fine estimation of delay time between emitted pulses and those received). This is achieved by correlating two consecutive segments of symbol-length received waveform, but this time in an interval that corresponds to the number of frames included in one data symbol. First, we applied this algorithm in single-user environments and then, have extended the used method in multi-user environments. Simulation results show that this new approach using TDT synchronizer can achieve a lower mean square error (MSE) than the original TDT for both NDA and DA synchronization mode.

The rest of this chapter is organized as follows. We describe our system model (PAM and PPM signals through time hopping spreading) with first stage synchronization (based on TDT) in Section 2, and then we give an outline of the well known TDT approach for UWB TH-PAM and TH-PPM impulse radios to better understand the overall timing synchronization in Section 3. In Section 4, we present the second step or stage of our synchronization approach with UWB time hopping systems in ad-hoc environments. The performance evaluation of our proposed fine synchronization approach with UWB TH-PAM and TH-PPM impulse radio systems in both single-user and multi-user environments is given in Section 5. And finally, we conclude this chapter in Section 6.

2. TH-PAM and TH-PPM UWB system model

Common multiple access techniques implemented for pulse based UWB systems are Time Hopping (TH) and Direct Sequence (DS). Appropriate modulation techniques include OOK (Foerster et al, 2001) and particularly PPM and PAM (Hämäläinen et al, 2002). A given UWB communication system will be a mixture of these techniques, leading to signals based on, for example, TH-PPM, TH-BPAM or DS-BPAM. TH-PAM and TH-PPM are almost certainly the most frequently adopted scheme and will be applied in the following as an example for determining the resources existing in a UWB system in single-user and multi-user environments.

2.1 TH-PAM UWB system model for single-user links

In UWB impulse radios, each information symbol is transmitted over a T_s period that consists of N_f frames (Win & Sholtz, 2000). During each frame of duration T_f, a data-modulated ultra-short pulse p(t) with duration $T_p \ll T_f$ is transmitted from the antenna source. The transmitted signal is

$$v(t) = \sqrt{\varepsilon}\sum_{k=0}^{+\infty}\tilde{s}(k)\sum_{i=0}^{N_f-1}p(t - iT_f - c_{th}(i)T_c - kT_s) \quad (1)$$

where ε is the energy per pulse. $\tilde{s}(k) \coloneqq s(k)\tilde{s}(k-1)$ are differentially encoded symbols and drawn equiprobably from a finite alphabet. In our case, s(k) are denoting the binary PAM information symbols. User separation is realized with pseudo-random TH-codes $c_{th}(i)$, which time-shift the pulse positions at multiples of the chip duration T_c (Win & Sholtz, 2000). In this paper, we focus on a single user link and treat multi-user interference (MUI) as noise.

The transmitted signal propagates through the multipath channel with impulse response

$$g(t) = \sum_{l=0}^{L-1}\alpha_l\delta(t - \tau_l) \quad (2)$$

where $\{\alpha_l\}_{l=0}^{L-1}$ and $\{\tau_l\}_{l=0}^{L-1}$ are amplitudes and delays of the L multipath elements, respectively. The channel is assumed quasi-static and among $\{\tau_l\}_{l=0}^{L-1}$, τ_0 represents the propagation delay of the channel.

Then, the received waveform is given by

$$r(t) = \sqrt{\varepsilon}\sum_{k=0}^{+\infty}\tilde{s}(k)p_T(t - kT_s - \tau_{l,0} - \tau_0) + \eta(t) \quad (3)$$

where $\tau_{l,0}$ is arbitrary reference at the receiver representing the delay relative to the arrival moment of the first pulse, $\eta(t)$ is the additive noise and $p_T(t)$ denotes the received symbol waveform as

$$p_T(t) = \sum_{i=0}^{N_f-1}p(t - iT_f - c_{th}(i)T_c) * g(t + \tau_0) \quad (4)$$

where * indicates the convolution operation. We define the timing offset as $\Delta\tau \coloneqq \tau_{l,0} - \tau_0$. Let us suppose that $\Delta\tau$ is in the range of $[0, T_s)$ and we will show in the rest of this paper that this assumption will not affect the timing synchronization.

2.2 TH-PPM UWB system model for single-user links

With PPM modulation (Durisi & Benedetto, 2003; Di Renzo et al, 2005), the transmitted signal in single-user links is described by the following model

$$v(t) = \sqrt{\varepsilon}\sum_{k=0}^{+\infty}\sum_{i=0}^{N_f-1} p(t - iT_f - c_{th}(i)T_c - kT_s - d_i\delta) \quad (5)$$

where ε is the energy per pulse, $d_i \in (0,1)$ represents the i-th information bit transmitted, and δ is the time shift associated with binary PPM. User separation is realized with pseudo-random TH-codes $c_{th}(i)$, which time-shift the pulse positions at multiples of the chip duration T_c (Win & Sholtz, 2000). In this paper, we focus on a single user link and treat multi-user interference (MUI) as noise.

After the transmitted signal propagation through the multipath channel, the received waveform is given by

$$r(t) = \sqrt{\varepsilon}\sum_{l=0}^{L}\alpha_l\sum_{k=0}^{+\infty} p_T\left(t - kT_s - \tau_{l,0} - \tau_0 - d_i\delta\right) + \eta(t) \quad (6)$$

where $\tau_{l,0}$ is arbitrary reference at the receiver representing the delay relative to the arrival moment of the first pulse, η(t) is the additive noise and $p_T(t)$ denotes the received symbol waveform as

$$p_T(t) = \sum_{i=0}^{N_f-1} p(t - iT_f - c_{th}(i)T_c) * g(t + \tau_0) \quad (7)$$

where * indicates the convolution operation. We define the timing offset as $\Delta\tau := \tau_{l,0} - \tau_0$. Let us suppose that Δτ is in the range of $[0, T_s)$ and we will show in the rest of this paper that this assumption will not affect the timing synchronization. Let $p_R(t)$ the overall received symbol-long waveform defined as follows

$$p_R(t) = \sum_{l=0}^{L}\alpha_l p_T\left(t - \tau_{l,0}\right) \quad (8)$$

Using (8), the received waveform in (6) becomes

$$r(t) = \sqrt{\varepsilon}\sum_{k=0}^{+\infty} p_R(t - kT_s - \tau_0 - d_i\delta) + \eta(t) \quad (9)$$

2.3 TH-PAM UWB system model for single-user links

The UWB time hopping impulse radio signal considered in this paper is a stream of narrow pulses, which are shifted in amplitude modulated (PAM). The transmitted waveform from the *u*th user is

$$v_u(t) = \sqrt{\varepsilon_u}\sum_{k=0}^{+\infty} s_u(k)p_{u,T}(t - kT_s) \quad (10)$$

where ε_u represents the energy per pulse, $s_u(k)$ are differentially encoded symbols and drawn equiprobably from finite alphabet. In our case, $s_u(k)$ symbolize the binary PAM information symbols and $p_{u,T}(t)$ indicates the transmitted symbol

$$p_{u,T}(t) := \sum_{i=0}^{N_f-1} p(t - iT_f - c_u(i)T_c) \quad (11)$$

where T_c is the chip duration and $c_u(i)$ is the user-specific pseudo-random TH code during the *i*th frame.

After the transmitted signal propagation through the multipath channel, the received waveform from all users is

$$p_{u,T}(t) := \sum_{i=0}^{N_f-1} p(t - iT_f - c_u(i)T_c) \quad (12)$$

where N_u is the user's number, τ_u is the propagation delay of the *u*th user's direct path and $\eta(t)$ is the zero-mean additive Gaussian noise (AGN). The global received symbol-long waveform is therefore given by

$$p_{u,R}(t) := \sum_{l=0}^{L_u-1} \alpha_{u,l} p_{u,T}(t - \tau_{u,l}) \quad (13)$$

Assuming that the nonzero support of waveform $p_{u,R}(t)$ is upper bounded by the symbol time T_s, the received waveform in (3) can be rewritten as

$$r(t) = \sum_{u=0}^{N_u-1} \sqrt{\varepsilon_u} \sum_{k=0}^{+\infty} s_u(k) p_{u,R}(t - kT_s - \tau_u) + \eta(t) \quad (14)$$

3. TDT approach

As mentioned previously, our proposed timing scheme consists of two complementary floors or steps. The first is based on a coarse (or blind) synchronization that is TDT developed in (Yang & Giannakis, 2005). In this section, we will give an outline of the TDT approach to better understand the overall timing synchronization suggested in this paper. The general structure description of our system model with first stage synchronization (TDT) is illustrated in Fig.1.

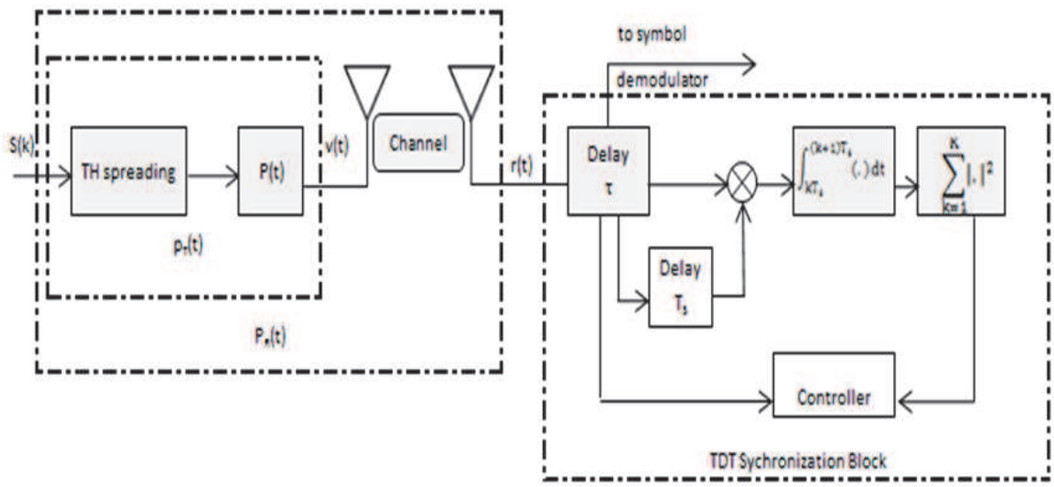

Fig. 1. Description of our model with first stage synchronization

The basic idea behind TDT is to find the maximum of square correlation between pairs of successive symbol-long segments. These symbol-long segments are called "dirty templates" because: i) they are noisy, ii) they are distorted by the unknown channel, and iii) they are subject to the unknown offset τ_0. Then, we will analyze $\widetilde{\tau_0}$ representing estimate offset of τ_0 by deriving upper bounds on their mean square error (MSE) in both non-data-aided (NDA) and data-aided (DA) modes.

3.1 TDT approach for TH-PAM UWB system in single-user links

For notational brevity and after setting $p_T(t) := p_R(t-\tau_{l,0})$, the received waveform simplifies to

$$r(t) = \sqrt{\varepsilon} \sum_{k=0}^{+\infty} \tilde{s}(k) p_R(t - kT_s - \tau_0) + \eta(t) \quad (15)$$

Thereafter, a correlation between the two adjacent symbol-long segments $r(t + kT_s)$ and $r(t + (k-1)T_s)$ is achieved. Let $x(k;\tau)$ the value of this correlation $\forall k \in [1, +\infty)$ and $\tau \in [0, T_s)$

$$x(k;\tau) = \int_0^{T_s} r(t + kT_s + \tau)\, r(t + (k-1)T_s + \tau)dt \quad (16)$$

Applying the Cauchy-Schwartz inequality and substituting the expressions of $r(t + kT_s)$ and $r(t + (k-1)T_s)$ to (16), $x(k;\tau)$ becomes

$$x(k;\tau) = \tilde{s}(k-1)[\,\tilde{s}(k-2)\,\varepsilon_A(\tilde{\tau_0}) + \tilde{s}(k)\,\varepsilon_B(\tilde{\tau_0})] + \zeta(k;\tau) \quad (17)$$

where $\varepsilon_A(\tau) \coloneqq \varepsilon \int_{T_s-\tau}^{T_s} p_R^2(t)dt$, $\varepsilon_B(\tau) \coloneqq \varepsilon \int_0^{T_s-\tau} p_R^2(t)dt$, and $\zeta(k;\tau)$ corresponds to the superposition of three noise terms (Yang & Giannakis, 2005) and can be approximated as an additive white Gaussian noise (AWGN) with zero mean and σ_ζ power.
By exploiting the statistical properties of the signal and noise, the mean square of the samples in (17) is given by

$$E\{x^2(k;\tau)\} = \frac{1}{2}\,[\varepsilon_A(\tilde{\tau_0}) + \varepsilon_B(\tilde{\tau_0})]2 + \frac{1}{2}\,[\varepsilon_A(\tilde{\tau_0}) - \varepsilon_B(\tilde{\tau_0})]2 + \sigma_\zeta^2 \quad (18)$$

We notice that $\varepsilon_B(\tilde{\tau_0}) + \varepsilon_A(\tilde{\tau_0}) = \varepsilon\int_0^{T_s} p_R^2(t)dt := \varepsilon_R$ for $\tilde{\tau_0} \in [0, T_s)$, where ε_R represents the constant energy corresponding to the unknown aggregate template at the receiver. Then the mean square of $x^2(k;\tau)$ can be rewritten as follows

$$E\{x^2(k;\tau)\} = \frac{1}{2}\,(\varepsilon_R)^2 + \frac{1}{2}\,[2\varepsilon_A(\tilde{\tau_0}) - \varepsilon_R]2 + \sigma_\zeta^2 \quad (19)$$

Since the term $\varepsilon_A(\tilde{\tau_0})$ reaches its unique maximum at $\tilde{\tau_0} = 0$, then $E\{x^2(k;\tau)\}$ also reached its unique maximum at $\tilde{\tau_0} = 0$. Thus, an estimate of timing offset τ_0 is given by

$$\hat{\tau}_0 = \arg max_{\tau\in[0,T_s]}\, E\{x^2(k;\tau)\} \quad (20)$$

In the practice, the mean square of $x^2(k;\tau)$ is estimated from the average of different values $x^2(k;\tau)$ for k ranging from 0 to M – 1 obtained during an observation interval of duration MT_s. In what follows, we summarize the TDT algorithm in its NDA form and then in its DA form.

3.1.1 Non-data-aided (blind) mode

For the synchronization mode NDA, the synchronization algorithm is defined as follows

$$\begin{cases} \hat{\tau}_{0,nda} = \arg max_{\tau\in[0,T_s]}\, E\{x^2(k;\tau)\} \\ x_{nda}(M;\tau) = \frac{1}{M}\sum_{m=0}^{M-1}\left(\int_{mT_s}^{(m+1)T_s} r(t+\tau)r(t+\tau+T_s)dt\right)^2 \end{cases} \quad (21)$$

By using (17), the expression of $x_{nda}(M;\tau)$ can be rewritten as follows

$$x_{nda}(M;\tau) = \frac{1}{M}\sum_{m=0}^{M-1}[s(m-1)s(m-2)\varepsilon_A(\tilde{\tau_0})\; s(m)s(m-1)\varepsilon_B(\tilde{\tau_0}) + \zeta(m;\tau)]^2 \quad (22)$$

From (19) and (20), the estimation of delay τ_0 is made possible due to the presence of the term $\varepsilon_A(\tilde{\tau_0})$ - $\varepsilon_B(\tilde{\tau_0})$. Unfortunately for the estimator $x_{nda}(M;\tau)$, this term exists only if the transmitted sequence presents an alternating sign between the symbols $s(m-2)$ and $s(m)$. Thus, for the synchronization in NDA mode, the performances of this approach are affected by the sign of the transmitted symbols. To increase the chances that the estimator $x_{nda}(M;\tau)$ is expressed as a function of the energy difference, an increase in the observation interval length is required. However, such an increase leads to increased acquisition delays. Where does the idea of using the data-aided (DA) approach.

3.1.2 Data-aided mode

The number of samples M required for reliable estimation can be reduced noticeably if a data-aided (DA) approach is pursued (Yang & Giannakis, 2003). The delays can be significantly reduced through the use of training sequences with alternating sign between the symbols $s(m-2)$ and $s(m)$, i.e. $s(m-2) = -s(m)$. This observation suggest that the training sequence $\{s(k)\}$ for DA TDT mode follows the following alternation $[1,1,-1,-1]$ (this by working with a M-ary PAM symbol); i.e.

$$s(k) = (-1)^{\left\lfloor \frac{k}{2} \right\rfloor} \tag{23}$$

This pattern is particularly attractive, since it simplifies the algorithm proposed by the TDT approach, for the DA mode, to become

$$\begin{cases} \hat{\tau}_{0,da} = \arg max_{\tau \in [0,T_s]} \{x_{da}(M;\tau)\} \\ x_{da}(M;\tau) = \left(\int_0^{T_s} r(t+\tau) r(t+\tau+T_s) dt\right)^2 \end{cases} \tag{24}$$

with

$$r(t) = \frac{2}{M} \sum_{k=0}^{\frac{M}{2}-1} (-1)^k r(t + 2kT_s + \tau).$$

The estimator in (24) is essentially the same as (22), except that training symbols are used in (24). However, theses training symbols are instrumental in improving the estimation performance. This will be approved by the simulation results.

3.2 TDT approach for TH-PPM UWB system in single-user links

For UWB TH-PPM systems, a correlation between the two adjacent symbol-long segments $r_k(t) = r(t + kT_s)$ and $r_{k+1}(t) = r(t + (k+1)T_s)$ is achieved (Yang, 2006). Let $x(k;\tau)$ the value of this correlation $\forall k \in [1, +\infty)$ and $\tau \in [0, T_s)$

$$\begin{cases} x(k;\tau) \coloneqq \int_0^{T_s} r_{k+1}(t;\tau)\, \tilde{r}_k(t;\tau) dt \\ \tilde{r}_k(t;\tau) \coloneqq r_k(t+\delta;\tau) - r_k(t-\delta;\tau) \end{cases} \tag{25}$$

By applying the Cauchy-Schwartz inequality and exploiting the statistical properties of the signal and noise (Yang, 2006), the mean square of the samples in (25) is given by

$$E_{s,\zeta}\{x^2(k;\tau)\} \approx \frac{1}{2}\left(\varepsilon_R^2 - 3\varepsilon_A(\tilde{\tau}_0)\varepsilon_B(\tilde{\tau}_0) + 2\sigma_\zeta^2\right) \tag{26}$$

where $\varepsilon_A(\tau) \coloneqq \varepsilon \int_{T_s-\tau}^{T_s} p_R^2(t) dt$, $\varepsilon_B(\tau) \coloneqq \varepsilon \int_0^{T_s-\tau} p_R^2(t) dt$, and σ_ζ is the power of $\zeta(k;\tau)$ corresponding to the superposition of three noise terms (Yang, 2006) and can be approximated as an additive white Gaussian noise (AWGN) with zero mean. We notice that $\varepsilon_B(\tilde{\tau}_0) + \varepsilon_A(\tilde{\tau}_0) = \varepsilon \int_0^{T_s} p_R^2(t) dt := \varepsilon_R$ for $\tilde{\tau}_0 \in [0, T_s)$, where ε_R represents the constant energy corresponding to the unknown aggregate template at the receiver.

Similarly to PAM signals, the term $E_{s,\zeta}\{x^2(k;\tau)\}$ reached its unique maximum at $\tilde{\tau}_0 = 0$. In the practice, the mean square of $x^2(k;\tau)$ is estimated from the average of different values $x^2(k;\tau)$ for k ranging from 0 to M – 1 obtained during an observation interval of duration MT_s. In what follows, we summarize the TDT algorithm for UWB TH-PPM systems in its NDA form and then in its DA form.

3.2.1 Non-data-aided mode

For the synchronization mode NDA, the synchronization algorithm is defined as follows

$$\begin{cases} \hat{\tau}_{0,\mathrm{nda}} = \arg\max_{\tau\in[0,T_s]} x_{\mathrm{nda}}(M;\tau) \\ x_{\mathrm{nda}}(M;\tau) = \frac{1}{M}\sum_{m=0}^{M-1}\left(\int_0^{T_s} r_k(t;\tau)\tilde{r}_{k-1}(t;\tau)dt\right)^2 \end{cases} \tag{27}$$

The estimator $\hat{\tau}_{0,\,\mathrm{nda}}$ in (27) can be verified to be m.s.s. consistent by deriving the mean and variance of the function $x_{\mathrm{nda}}(M;\tau)$ (Yang, 2006).

3.2.2 Data-aided mode

For UWB TH-PPM, the training sequence for DA TDT is considered to comprise a repeated pattern (for example (1,0, 1,0)); that is.

$$s(k) = \{k+1\}_2 \tag{28}$$

With this pattern, it can be easily verified that the mean square in (26) becomes

$$E_{s,\zeta}\{x^2(k;\tau)\} = \varepsilon_R^2 - 4\varepsilon_A(\widetilde{\tau_0})\varepsilon_B(\widetilde{\tau_0}) + \sigma_\zeta^2 \tag{29}$$

With the NDA approach, it is necessary to take expectation with respect to s_k in order to remove the unknown symbol effects; while the DA mode, this is not needed. Hence, the sample mean $M^{-1}\sum_{m=0}^{M-1}x^2(k;\tau)$converges faster to its expected value in (29). This pattern is particularly attractive, since it permits a very rapid acquisition which is a major benefit of the DA mode. Data-aided TDT for UWB TH-PPM signals can be accomplished even when TH codes are present and the multipath channel is unknown, using

$$\begin{cases} \hat{\tau}_{0,\mathrm{da}} = \arg\max_{\tau\in[0,T_s]} x_{\mathrm{da}} \\ x_{\mathrm{da}}(M;\tau) = \left(\frac{1}{M}\sum_{m=0}^{M-1}\int_0^{T_s} r_k(t;\tau)\tilde{r}_{k-1}(t;\tau)dt\right)^2 \end{cases} \tag{30}$$

The estimator in (30) is essentially the same as (27), except training symbols used in (30). However, theses training symbols are essential in improving the estimation performance. This will be approved by the simulation results.

3.3 TDT approach for TH-PAM UWB system in multi-user links

For multi-user UWB TH-PAM systems, a correlation between the two adjacent symbol-long segments $r(t-kT_s)$ and $r(t-(k-1)T_s)$ is achieved. Let $x(k;\tau)$ the value of this correlation $\forall k \in [1,+\infty)$ and $\tau \in [0,T_s)$

$$x(k;\tau) = \sum_{u=0}^{N_u-1}\int_0^{T_s} r(t-kT_s)r(t-(k-1)T_s)\,dt \tag{31}$$

Applying the Cauchy-Schwartz inequality and substituting the expressions of $r(t-kT_s)$ and $r(t-(k-1)T_s)$ to (31), $x(k;\tau)$ becomes

$$x(k;\tau) = \sum_{u=0}^{N_u-1} s_u(k-1)\left[s_u(k-2)\varepsilon_{u,A}(\tilde{\tau}_u) + s_u(k)\varepsilon_{u,B}(\tilde{\tau}_u)\right] + \xi(k;\tau) \tag{32}$$

where $\varepsilon_{u,A}(\tilde{\tau}_u) \coloneqq \varepsilon_u\int_{T_s-\tilde{\tau}_u}^{T_s} p_{u,R}^2(t)dt$, $\varepsilon_{u,B}(\tilde{\tau}_u) \coloneqq \varepsilon_u\int_0^{T_s-\tilde{\tau}_u} p_{u,R}^2(t)dt$, $\tilde{\tau}_u \coloneqq [\tau_u-\tau]_{T_s}$ and $\zeta(k;\tau)$ corresponds to the superposition of three noise terms (Yang & Giannakis, 2005) and can be approximated as an AWGN with zero mean and σ_ξ power. As mentioned in (Yang &

Giannakis, 2005), the noise-free part of the desired user's samples at the correlator output complies with

$$\chi_0(\mathrm{k};\tau) = \varepsilon_{0,\mathrm{A}}(\tilde{\tau}_0) - \varepsilon_{0,\mathrm{B}}(\tilde{\tau}_0) \tag{33}$$

Substituting the above equation into (31), we find

$$\mathrm{x}(\mathrm{k};\tau) = \chi_0(\mathrm{k};\tau) + \sum_{\mathrm{u}\neq 0} \mathrm{s_u}(\mathrm{k}-1)\left[\mathrm{s_u}(\mathrm{k})\varepsilon_{\mathrm{u,B}}(\tilde{\tau}_\mathrm{u}) + \mathrm{s_u}(\mathrm{k}-2)\varepsilon_{\mathrm{u,A}}(\tilde{\tau}_\mathrm{u})\right] + \xi(\mathrm{k};\tau) \tag{34}$$

where $s_u(k)$'s are zero-mean information symbols emitted by the $(u \neq 0)$th user. If we calculate the average (without squaring), we obtain $E\{x(k;\tau)\} = \varepsilon_{0,B}(\tilde{\tau}_0) - \varepsilon_{0,A}(\tilde{\tau}_0)$ since $E\{\chi_u(k;\tau)\} = 0$ (Yang & Giannakis, 2005). In what follows, we summarize the TDT approach for multi-user UWB TH-PAM impulse radios in its NDA form and then in its DA form. .

3.3.1 Non-data-aided mode

For the NDA synchronization mode, the timing algorithm is defined as follows

$$\begin{cases} \hat{\tau}_{\mathrm{u,nda}} = \arg\max_{\tau\in[0,\mathrm{T_s}]} \mathrm{E}\{\mathrm{x}^2(\mathrm{k};\tau)\} \\ \mathrm{x_{nda}}(\mathrm{M};\tau_\mathrm{u}) = \frac{1}{\mathrm{M}}\sum_{\mathrm{m}=0}^{\mathrm{M}-1}\left(\mathrm{x}(\mathrm{k};\tau)\right)^2 \end{cases} \tag{35}$$

The estimator can be verified to be m.s.s consistent by deriving the mean and variance of $\mathrm{x_{nda}}(\mathrm{M};\tau_\mathrm{u})$. It has been demonstrated that the single-user TDT estimator is operational even in a multi-user environment (Yang & Giannakis, 2005).

3.3.2 Data-aided mode

The pattern described previously in (23) is particularly attractive, since it simplifies the proposed algorithm to become in the DA mode

$$\begin{cases} \hat{\tau}_{\mathrm{u,da}} = \arg max_{\tau\in[0,T_s]} \{\mathrm{x_{da}}(\mathrm{M};\tau)\} \\ \mathrm{x_{da}}(\mathrm{M};\tau) = \left(\int_0^{\mathrm{T_s}} \mathrm{r}(\mathrm{t}+\tau)\mathrm{r}(\mathrm{t}+\tau+\mathrm{kT_s})\mathrm{dt}\right)^2 \end{cases} \tag{36}$$

With $\mathrm{E}\left\{(-1)^{\left\lfloor\frac{k}{2}\right\rfloor}\mathrm{r}(\mathrm{t}+\tau+\mathrm{kT_s})\right\} = \sqrt{\varepsilon}\left[\mathrm{p_{0,R}}(\mathrm{t}+\mathrm{T_s}-\tilde{\tau}_0) + (-1)^\mathrm{k}\mathrm{p_{0,R}}(\mathrm{t}-\tilde{\tau}_0)\right]$ which signifies that the single-user TDT estimator can also be functional in a multi-user scenario.

4. Proposed fine synchronization approach

In this section, we will develop a low-complexity fine synchronization approach using TDT synchronizer in order to find the desired timing offset. The block diagram of our synchronization scheme is shown in Fig.2. Our approach will be evaluated in both NDA and DA modes, without knowledge of the multipath channel and the transmitted sequence (Hizem & Bouallegue, 2010; Hizem & Bouallegue, 2011, a; Hizem & Bouallegue, 2011, b).

This second floor achieves a fine estimation of the frame beginning, after a coarse research in the first. The concept which is based this floor is extremely simple. The idea is to scan the interval $[\tau_1 - \mathrm{T_{corr}},\ \tau_1 + \mathrm{T_{corr}}]$ with a step noted δ by making integration between the received signal and its replica shifted by $\mathrm{T_f}$ on a window of width $\mathrm{T_{corr}}$. τ_1 being the estimate delay deducted after the first synchronization floor and the width integration window

value's T_{corr} will be given in Section 5. This principle is illustrated in Fig.3. We can write the integration window output for the n^{th} step $n\delta$ as follows

$$Z_n = \sum_{k=0}^{K-1} \left| \int_{\tau_1+n\delta}^{\tau_1+n\delta+T_s} r(t - kT_s) r(t - (k+1)T_s) dt \right| \quad (37)$$

Where $n = -N+1..0..N-1$, $N = \lfloor T_{corr}/\delta \rfloor$ and K is number of frames considered for improving the decision taken at the first floor. The value of n which maximizes Z_n provides the exact moment of pulse beginning that we note $\tau_2 = \tau_1 + n_{opt}\delta$. Thus, the fine synchronization is performed. Finally, note that this approach will be applied in both NDA and DA modes with UWB TH-PAM and TH-PPM impulse radio systems for both single-user and multi-user environments. We will see later in what mode this approach gives better result compared to those given by the original approach TDT.

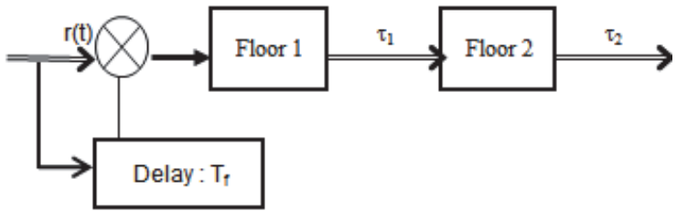

Fig. 2. Block diagram of our synchronization scheme

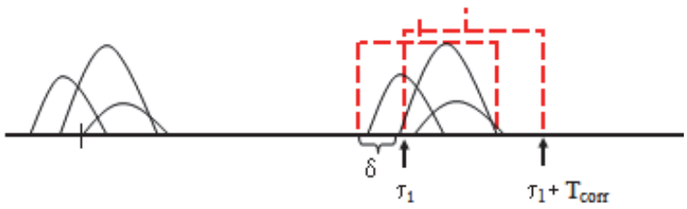

Fig. 3. Principle of second synchronization floor

5. Simulation results

In this section, we will evaluate the performance of our proposed fine synchronization approach with simulations. The UWB pulse is the second derivative of the Gaussian function with duration $T_p \approx 0.8$ns. Simulations are achieved in the IEEE 802.15.3a channel model CM1 (Foerster, 2002). The sampling frequency is f_c = 50 GHz. Each symbol contains N_f = 32 frames each with duration T_f = 35 ns. We used a random TH code over $[0, N_c - 1]$, with N_c = 35 and T_c = 1.0 ns. The width integration window value's T_{corr} is 4 ns. The performance of our synchronization approach is tested for various values of M.

5.1 TH-PAM UWB system in single-user links

In Fig. 4, we first test the MSE of NDA and DA TDT algorithms summarized in Section 3.1. The MSE is normalized by the square of the symbol duration T_s^2. From Fig.4, we note that increasing the duration of the observation interval M leads to improved performance for both NDA and DA modes. We also note that the use of training sequences (DA mode) leads to improved performance compared to the NDA mode.

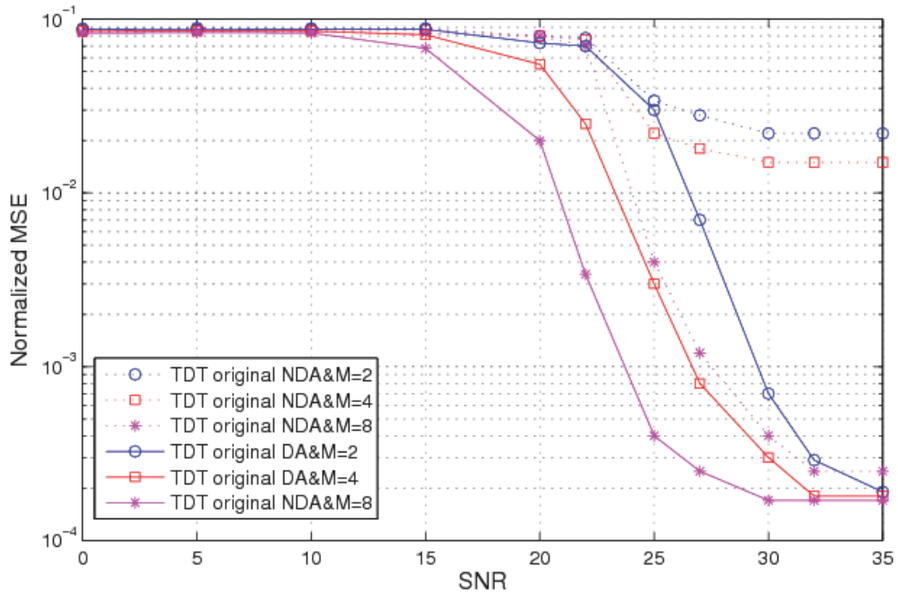

Fig. 4. Normalized MSE of the original TDT synchronizer in both NDA and DA modes

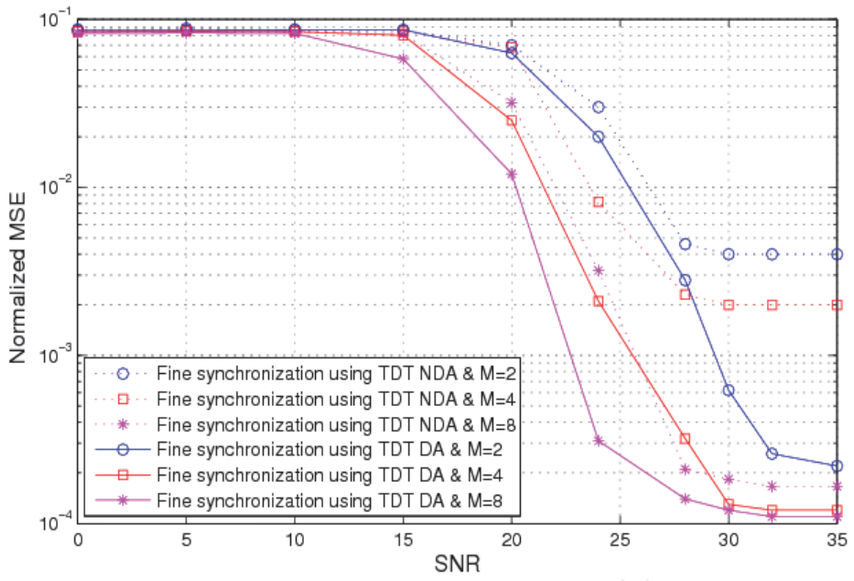

Fig. 5. Normalized MSE of our fine synchronization approach in both NDA and DA modes

In Figs. 5-7, we evaluate and compare by simulation the performance (in term of MSE) of our proposed fine synchronizer with the original NDA and DA TDT algorithms. In Fig. 5, we compare the performances of the new fine synchronization approach in both NDA and DA modes. In Fig. 6-7, we compare the performances of both original TDT and fine synchronization approach proposed for different values of M. In comparison with the original TDT approach, we note that the new approach outperforms the NDA mode and offers a slight improvement in DA mode. Even without any training symbol sequence, our synchronizer can greatly outperform the original NDA TDT especially when M is small.

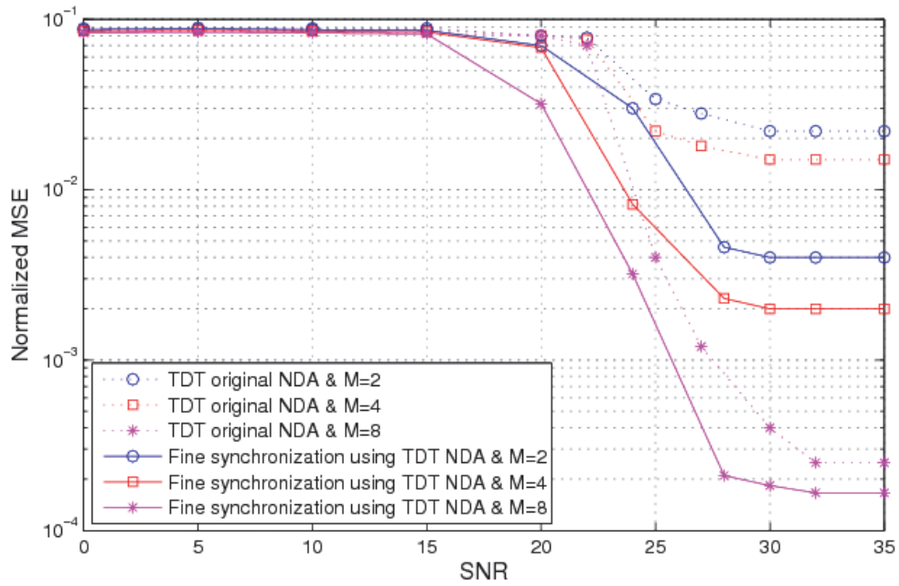

Fig. 6. Performances comparison between original TDT and our fine synchronization approaches in NDA mode

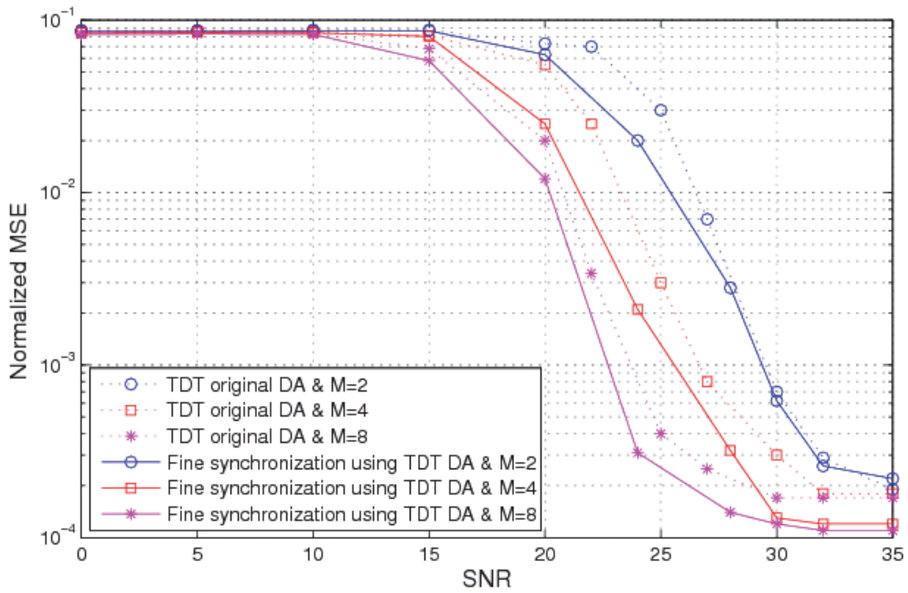

Fig. 7. Performances comparison between original TDT and our fine synchronization approaches in DA mode

5.2 TH-PPM UWB system in single-user links

In addition to other parameters described previously, the time shift associated with binary PPM is δ = 1ns. Then, the performance is tested for various values of M.

In Fig. 8, we first test the MSE of NDA and DA TDT algorithms for UWB TH-PPM systems. We note that increasing the duration of the observation interval M leads to improved

performance for both NDA and DA modes. We also note that the use of training sequences (DA mode) leads to improved performance compared to the NDA mode.

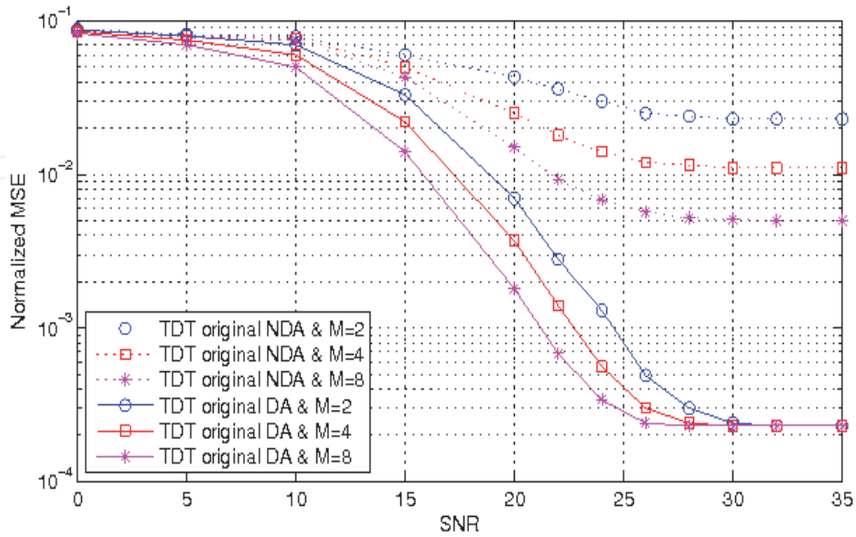

Fig. 8. Normalized MSE of TDT for UWB TH-PPM systems in both NDA and DA modes

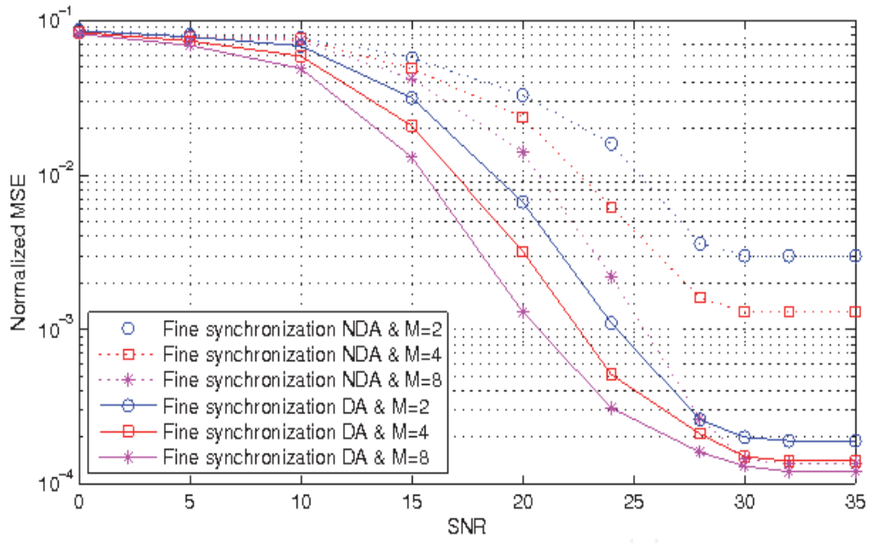

Fig. 9. Normalized MSE of our fine synchronization approach for UWB TH-PPM systems

In Figs. 9-11, we evaluate and compare by simulation the performance of our proposed fine synchronizer with the original TDT algorithms. In Fig. 9, we compare the performances of the new fine synchronization approach in both NDA and DA modes. In Fig. 10-11, we compare the performances of both original TDT and fine synchronization approach proposed in both NDA and DA modes for different values of M. In comparison with the original TDT approach, we note that the new approach outperforms the NDA mode and offers a slight improvement in DA mode. Even without any training symbol sequence, our synchronizer can greatly outperform the original NDA TDT especially when M is small.

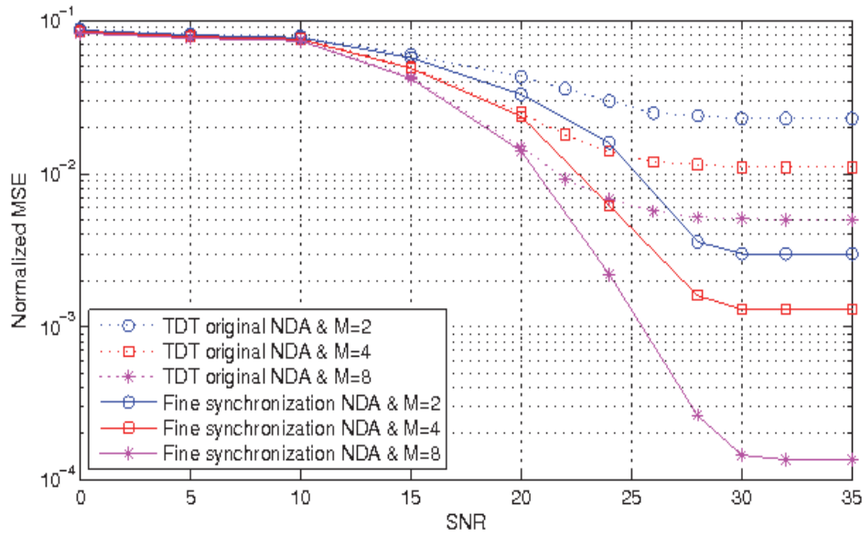

Fig. 10. Performances comparison between original TDT and our fine synchronization approaches for UWB TH-PPM systems in NDA mode

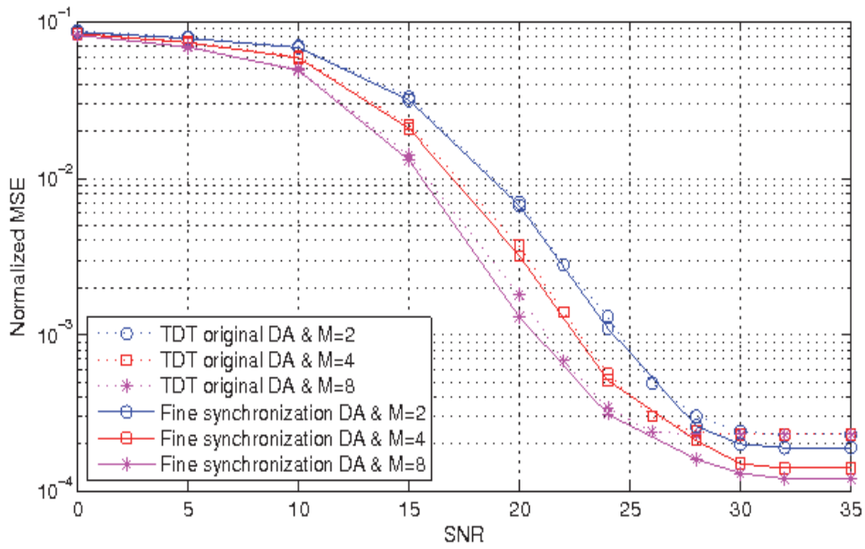

Fig. 11. Performances comparison between original TDT and our fine synchronization approaches for UWB TH-PPM systems in DA mode

5.3 TH-PAM UWB system in multi-user links

In this part, we will evaluate the performance of our proposed fine synchronization approach for UWB TH-PAM signals in ad-hoc multi-user environments. The performance is tested for various values of M.

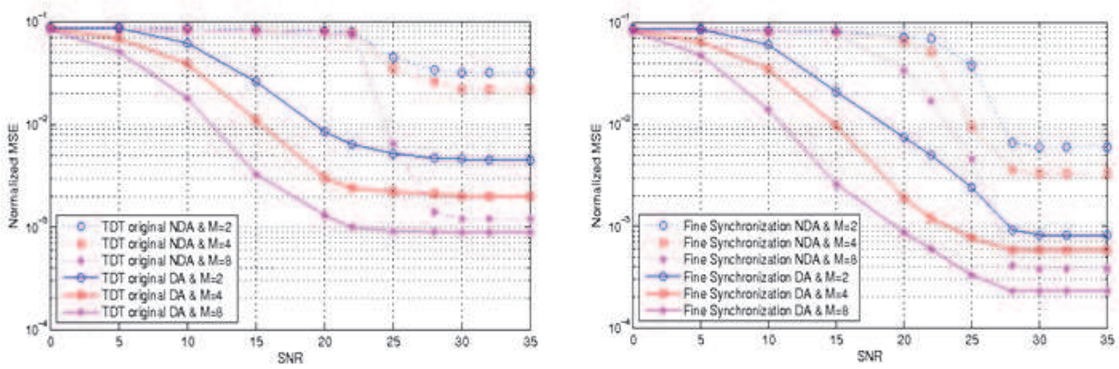

Fig. 12. Normalized MSE of multi-user original TDT synchronizer and our multi-user fine synchronization

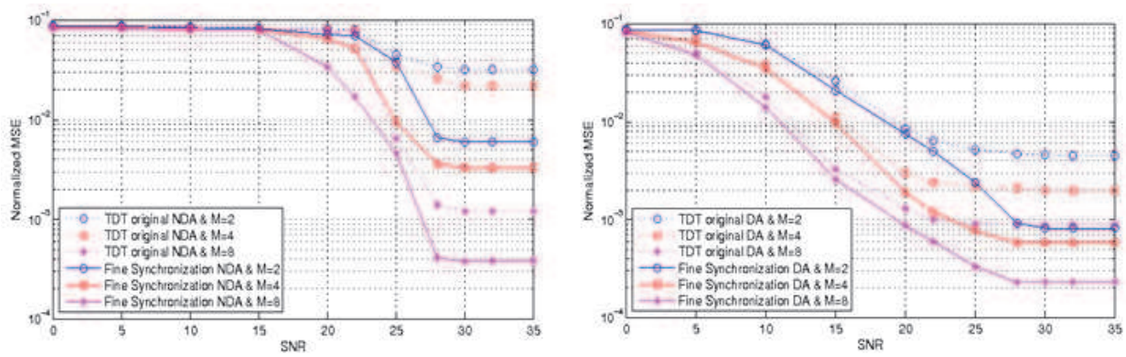

Fig. 13. Performances comparison in NDA and DA modes with multi-user environments

In Fig. 12 on left, we first test the mean square error (MSE) corresponding to (35) and (36). From the simulation results, we note that increasing the duration of the observation interval M leads to improved performance for both NDA and DA modes. We also note that the use of training sequences (DA mode) leads to improved performance compared to the NDA mode. In Fig. 12 on right, we compare the new fine synchronization approach performances in both NDA and DA modes. In Fig. 13, we compare the performances of both original TDT and fine synchronization approach for different values of M. In comparison with the original TDT approach, we note that the new approach greatly outperforms the NDA mode and offers a slight improvement in DA mode. This performance improvement is enabled at the price of fine synchronization approach introduced in second floor which can further improve the timing offset found in first floor.

6. Conclusion

In this chapter, we have discussed the problem of UWB system performance in single-user and multi-user environments. While there is a rich body of literature addressing this problem most of which has emerged recently, this topic is far from being mature. In this context, developing novel approaches with relatively low complexity still represents crucial task in meeting the challenges of UWB communications.

We first describe the TH-PAM and TH-PPM UWB system model in single-user and multi-user environments. Then, we give an outline of the TDT approach. In the rest of this chapter, we propose a novel fine synchronization scheme using TDT algorithm for UWB TH-PAM and TH-PPM radio system in single-user and multi-user links. With the introduced fine synchronization algorithm, we can achieve a fine estimation of the frame beginning. The performance improvement is enabled at the price of fine synchronization approach introduced in second floor which can further improve the timing offset found in first floor (coarse synchronization approach : TDT). The simulation results show that even without training symbols, our new synchronizer can enable a better performance than the original TDT in NDA mode especially when M is small and offers a slight improvement in DA mode.

7. References

Carbonelli, C.; Mengali, U. & Mitra, U. (2003). Synchronization and channel estimation for UWB signals, *Proceedings of GLOBECOM Conference*, San Francisco, CA, vol. 2, pp. 764-768, December 1-5, 2003

Dang, Q. H.; Trindade, A. & Van der Veen, A. J. (2006). Signal model and receiver algorithms for a Transmit-Reference Ultra-Wideband Communication system, *Proceedings of IEEE Journal of Selected Areas in Communications*, vol. 24, No. 4, pp. 773-779, April 2006

Djapic, R.; Leus, G.; Van der Veen, A. J. & Trindade, A. (2006). Blind synchronization in asynchronous UWB networks based on the transmit-reference scheme, *Proceedings of EURASIP Journal on Wireless Communications and Networking*, vol. 2006, No. 2, pp. 65-75, April 2006

Di Renzo, M.; Graziosi, F. & Santucci, F. (2005). A framework for performance analysis for TH-UWB communications, *Proceedings of IEEE International Conference on Ultra-Wideband (ICUWB)*, Zurich, Switzerland, pp. 559-564, September 5-8, 2005

Durisi, G. & Benedetto, S. (2003). Performance evaluation of TH-PPM UWB systems in the presence of multi-user interference, *Proceedings of IEEE Communication Letters*, vol. 5, pp. 224-226, May 2003

Fleming, R.; Kushner, C.; Roberts, G. & Nandiwada U. (2002). Rapid acquisition for ultra-wideband localizers, *Proceedings of Conference on Ultra-Wideband System Technologies*, Baltimore, MD, pp. 245-250, May 20-23, 2002

Foerster, J. R.; Green, E.; Somayazulu, S. & Leeper, D. (2001) Ultra-Wideband Technology for short or medium range wireless communications, *Intel Technology Journal*, Q2, 11p

Foerster, J. R. (2002) Channel Modelling Sub-committee Report Final, *IEEE P802.15-02/368r5-SG3a*, *IEEE P802.15 Working Group for WPAN*, November 2002

Hämäläinen, M.; Hovinen, V. & Latva-aho, M. (2002) On the UWB System Coexistence with GSM900, UMTS/WCDMA and GPS, *IEEE Journal on Selected Areas in Communications*, Vol. 20, No. 9, (Dec. 2002), pp. 1712-1721, ISSN 0733-8716

Hizem, M. & Bouallegue, R. (2010) Novel Fine Synchronization Using TDT for Ultra Wideband Impulse Radios, *Proceedings of International Information and Telecommunication Technologies Symposium (I2TS)*, Botafogo, Rio de Janeiro, Brazil, December 13-15, 2010

Hizem, M. & Bouallegue, R. (2011a) Fine Synchronization through UWB TH-PPM Impulse Radios, *Proceedings of International Journal of Wireless & Mobile Networks (IJWMN) Vol. 3, No. 1, February 2011*

Hizem, M. & Bouallegue, R. (2011b) Fine Synchronization with UWB TH-PAM Signals in ad-hoc Multi-user Environments, *Proceedings of Progress in Electromagnetics Research Symposium (PIERS)*, Marrakech, Morocco, March 20-23, 2011

Homier, E. A. & Schloltz, R. A. (2002). Rapid acquisition for ultra-wideband signals in the dense multipath channel, *Proceedings of Conference on Ultra-Wideband System Technologies*, Baltimore, MD, pp. 105-110, May 20-23, 2002

Lottici, V.; Andrea, A. D. & Mengali, U. (2002). Channel estimation for ultra wideband communications, *Proceedings of IEEE Journal of Selected Areas in Communications*, vol. 20, pp. 1638-1645, December 2002

Tian, Z. & Giannakis, G. B. (2003). Data-aided ML timing acquisition in ultra-wideband radios, *Proceedings of Conference on Ultra-Wideband System Technologies*, Reston, VA, pp. 245-250, November 16-19, 2003

Tian, Z. & Giannakis, G. B. (2005). BER sensitivity to mistiming in ultra-wideband communications-Part I: Non-random channels, *Proceedings of IEEE on Signal Processing,* vol. 53, No. 4, pp. 1550-1560, April 2005

Yang, L. & Giannakis, G. B. (2003). Low-complexity training for rapid timing synchronization in ultra-wideband communications, *Proceedings of Global Telecommunications Conference,* San Francisco, CA, pp. 769-773, December 2003

Yang, L.; Tian, Z. & Giannakis, G. B. (2003). Non-data aided timing acquisition of ultra-wideband transmissions using cyclostationarity, *Proceedings of International Conference in Acoustics, Speech, Signal Processing*, Hong Kong, China, pp. 121-124, April 6-10, 2003

Yang, L. & Giannakis, G. B. (2004). Ultra-wideband communications: an idea whose time has come, *Proceedings of IEEE on Signal Processing Magazine,* vol. 21, No. 6, pp. 26-54, November 2004

Yang, L. & Giannakis, G. B. (2005). Timing UWB signals using dirty templates, *Proceedings of IEEE Transactions on Communications,* vol. 53, No. 11, pp. 1952-1963, November 2005

Yang, L. (2006). Timing PPM-UWB signals in ad hoc multi-access, *Proceedings of IEEE Journal of Selected Areas in Communications*, vol. 24, No. 4, pp. 794-800, April 2006

Ying, Y.; Ghogho, M. & Swami, A. (2008). Code-Assisted synchronization for UWB-IR systems: algorithms and analysis, *Proceedings of IEEE Transactions on Signal Processing*, vol. 56, No. 10, pp. 5169-5180, October 2008

Win, M. Z. & Scholtz, R. A. (2000). Ultra wide bandwidth time-hopping spread-spectrum impulse radio for wireless multiple access communications, *Proceedings of IEEE Transactions on Communications*, vol. 48, No. 4, PP. 679-691, April 2000

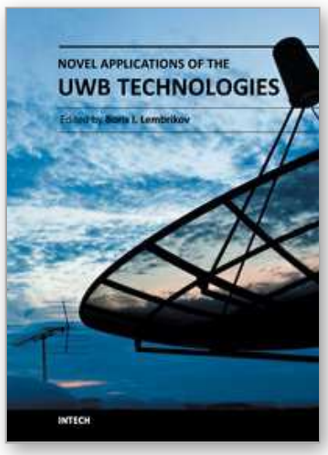

Novel Applications of the UWB Technologies

Edited by Dr. Boris Lembrikov

ISBN 978-953-307-324-8
Hard cover, 440 pages
Publisher InTech
Published online 01, August, 2011
Published in print edition August, 2011

Ultra wideband (UWB) communication systems are characterized by high data rates, low cost, multipath immunity, and low power transmission. In 2002, the Federal Communication Commission (FCC) legalized low power UWB emission between 3.1 GHz and 10.6 GHz for indoor communication devices stimulating rapid development of UWB technologies and applications. The proposed book Novel Applications of the UWB Technologies consists of 5 parts and 20 chapters concerning the general problems of UWB communication systems, and novel UWB applications in personal area networks (PANs), medicine, radars and localization systems. The book will be interesting for engineers and researchers occupied in the field of UWB technology.

INTECH
open science | open minds

InTech Europe
University Campus STeP Ri
Slavka Krautzeka 83/A
51000 Rijeka, Croatia
Phone: +385 (51) 770 447
Fax: +385 (51) 686 166
www.intechopen.com

InTech China
Unit 405, Office Block, Hotel Equatorial Shanghai
No.65, Yan An Road (West), Shanghai, 200040, China
中国上海市延安西路65号上海国际贵都大饭店办公楼405单元
Phone: +86-21-62489820
Fax: +86-21-62489821

IntechOpen